

Pomeron evolution, entanglement entropy and Abramovskii-Gribov-Kancheli cutting rules

Mustapha Ouchen and Alex Prygarin
Department of Physics, Ariel University, Ariel 40700, Israel

Abstract

We use Pomeron evolution equation in zero transverse dimension based on the Abramovskii-Gribov-Kancheli (AGK) cutting rules to calculate the von Neumann entropy and q -moments that used as an experimental test for the Koba-Nielsen-Olesen (KNO) scaling. In order to avoid the negative probabilities that emerge from the negative AGK weights in the Minkowski space, we reformulate the Pomeron evolution in the Euclidean space. The resulting positive definite probabilities for cut and uncut Pomerons are used in calculating the q -moments. The comparison to the experimental data shows that our AGK based model successfully describes q -moments dependence on the mean multiplicity without any adjustable parameter in the experimental data of the $p - p$ collisions by ALICE Collaboration.

1 Introduction

In this paper we apply the analysis done by Levin and one of the authors [1] using the Abramovskii-Gribov-Kancheli [2] rules and derive the von Neumann entropy for studying the entanglement in the high energy scattering. This continues the project started by Levin and Kharzeev [3] which initiated a lot of activity related to that topic [4–17], other QCD related studies [18–32] and beyond [33–44].

Our goal is to build a simple model without free adjustable parameters, which will successfully describe the experimental data with emphasis on the violation of the Koba-Nielsen-Olesen (KNO) scaling [45].

In the first section we start with review of Kharzeev-Levin (KL) model [3] in zero transverse dimension defining the von Neumann entropy applied to the Pomeron evolution and the moments C_q that can be directly compared to the experimental data.

In the next section we review the Pomeron evolution equation based on the AGK cutting rules developed by Levin and one of the authors [1] (see also [46–48]) and discuss negative probabilities which arise in this context. The negative probabilities originate from the negative AGK weights of the relative contributions to the total cross section and related to the fact that the AGK cutting rules are derived in the Minkowski space. We reformulate

the Pomeron evolution in the Euclidean space based on the combinatorial considerations used in the original AGK cutting rules. The resulting evolution equation correctly reflects the positive definite probabilities of having cut and uncut Pomerons as a function of rapidity. Using the AGK based positive definite probabilities we construct the von Neumann entropy and calculate C_q as function of rapidity and the mean multiplicity of the produced particles.

Our model based on the AGK cutting rules successfully describes the C_q as a function of the mean multiplicity of the produced particles in the experimental data of the $\text{p} - \text{p}$ collision by ALICE Collaboration [49] without any adjustable parameter.

In the last section we summarize and discuss our results.

2 Toy model at zero transverse dimension

In this section we follow the lines of the dipole evolution analysis for the entanglement in QCD done by Kharzeev and Levin [3]. In this paper we use Pomeron as the proper degree of freedom and adopt the notation of the paper by Levin and one of the authors [1]. It is convenient to define the generating function

$$Z_0(u|Y) = \sum_{n=1}^{\infty} P_n(Y) u^n. \quad (1)$$

that introduces $P_n(Y)$, the probability of having n Pomerons at a given rapidity Y . The definition of the generating function implies that

$$Z_0(u = 1|Y) = 1 \quad (2)$$

if the total probability is properly normalized.

The Markov chain equation for the Pomeron evolution reads

$$\frac{\partial P_n(Y)}{\partial Y} = -\alpha n P_n(Y) + \alpha(n-1) P_{n-1}(Y) \quad (3)$$

The equation in (3) can be written as

$$\frac{\partial Z_0(u|Y)}{\partial Y} = -\alpha u(1-u) \frac{\partial Z_0(u|Y)}{\partial u} \quad (4)$$

where α denotes the Pomeron splitting vertex. This evolution equation is solved for the initial condition

$$Z_0(u|Y = 0) = u \quad (5)$$

that corresponds to starting with one Pomeron at $Y = 0$. The solution of (4) given by

$$Z_0(u|Y) = \frac{u}{u + (1 - u)e^{\alpha Y}} \quad (6)$$

satisfies the initial condition in (5) and the boundary condition in (2). Using the definition of $Z_0(u|Y)$ in (1) one can extract the probability $P_n(Y)$ of having n Pomerons at rapidity Y

$$P_n(Y) = e^{-\alpha Y} (1 - e^{-\alpha Y})^{n-1} \quad (7)$$

It is worth emphasizing that $P_n(Y)$ in (7) represents the probability of the *Geometric Distribution* also known as the *Furry Distribution* [51]

$$\Pr(\mathbf{X} = \mathbf{k}) = p (1 - p)^{k-1}, \quad k = 1, 2, 3, \dots \quad (8)$$

$\Pr(\mathbf{X} = \mathbf{k})$ stands for the probability of having the first occurrence of success after k independent trials in the Bernoulli process, each with success probability p . The Geometric Distribution is the only discrete probability distribution which is *memoryless*, i.e. previous fails does not affect future trials required for success. Another interesting property of the Geometric Distribution relevant for our discussion is that out of all possible known discrete probability distributions it gives the maximal entropy for the same set of parameters. The Bernoulli process is the process of having equally distributed binary variable (0- "fail" and 1-"success"). In our case, the meaning of "fail" is the absence of Pomeron at rapidity Y , where it potentially could be if we had only splitting at each stage of evolution (the $u^2 \frac{\partial}{\partial u}$ term in (4)). The $u \frac{\partial}{\partial u}$ term in (4) is responsible for propagation of a Pomeron without splitting thus introducing a "vacancy" or the absence of a Pomeron, which we recognize as "fail" with probability $q = 1 - p$, where $p = e^{-\alpha Y}$.

The mean number of Pomerons at rapidity Y is given by

$$\langle n \rangle = \sum_{n=1}^{\infty} n P_n(Y) = e^{\alpha Y} \quad (9)$$

which can be used to express the probability in (7) in terms of $\langle n \rangle$

$$P_n \left(Y = \frac{\ln \langle n \rangle}{\alpha} \right) = (\langle n \rangle - 1)^{n-1} \langle n \rangle. \quad (10)$$

The useful measure of disorder or uncertainty of the system is the entropy. There are a lot of expressions for entropy derived based on its definition in the classical thermodynamics. We adopt the von Neumann entropy

$$S = - \sum_{n=1}^{\infty} P_n(Y) \ln P_n(Y) \quad (11)$$

which measures the statistical uncertainty of quantum systems. Plugging the probability in (7) we obtain

$$S = \alpha Y e^{\alpha Y} - (e^{\alpha Y} - 1) \log(e^{\alpha Y} - 1), \quad (12)$$

which is a large rapidity can be approximated by

$$S \simeq \alpha Y + 1 - \frac{e^{-\alpha Y}}{2} = \ln \langle n \rangle + 1 - \frac{1}{2 \langle n \rangle}. \quad (13)$$

The fact that the entropy equals the log of the mean number of Pomeron states indicates that at $Y \rightarrow \infty$ the system is in the most entangled state. It is convenient to introduce a universal measure of uncertainty that can be used for comparison of various systems with different degrees of freedom or alternative states.

Inspired by the *efficiency index* for communication channels in the work of Wilcox [50] we introduce the *uncertainty index*

$$\eta(Y) = \frac{S}{\ln \langle n \rangle} = \frac{- \sum_{n=1}^{\infty} P_n(Y) \ln P_n(Y)}{\ln \langle n \rangle} \quad (14)$$

which measures the uncertainty (entropy) of the system normalized by $\ln \langle n \rangle$ where $\langle n \rangle$ is the average number of Pomerons at a given rapidity Y . In other words, one defines $\eta(Y)$ as a relative uncertainty or *the uncertainty indicator*¹ that indicates to which extent different alternatives in the system are equally likely. In the limiting case of the absolute certainty, i.e. all alternative states are equally likely, the uncertainty index $\eta(Y)$ approaches unity from above. For $\eta(Y) = 1$ all alternative states has the same probability, which makes the system less diverse and thus more certain with maximal entanglement. The uncertainty index $\eta(Y)$ in (14) can be viewed as a

¹The original name *the uncertainty index* of $\eta(Y)$ relates to the efficiency of data transfer in the information science and could be misleading in our case. Note also the difference in definition of $\eta(Y)$ where we use $\langle n \rangle$ instead of total number of alternatives in the information science.

reasonable entanglement measure for relative comparison of quite different systems.

For the probability given in (7) it reads

$$\eta(Y) = e^{\alpha Y} - \frac{(e^{\alpha Y} - 1) \ln(e^{\alpha Y} - 1)}{\alpha Y} = 1 - \frac{1 - e^{-\alpha Y}}{e^{-\alpha Y}} \frac{\ln(1 - e^{-\alpha Y})}{\alpha Y} \quad (15)$$

The plot of $\eta(Y)$ depicted in Figure 2 demonstrates convergence of the uncertainty index to unity at large rapidity

$$\eta(Y) \simeq 1 + \frac{1}{\alpha Y} - \frac{e^{-\alpha Y}}{2\alpha Y} = 1 + \frac{1}{\ln\langle n \rangle} - \frac{1}{2\langle n \rangle \ln\langle n \rangle}, \quad Y \rightarrow \infty \quad (16)$$

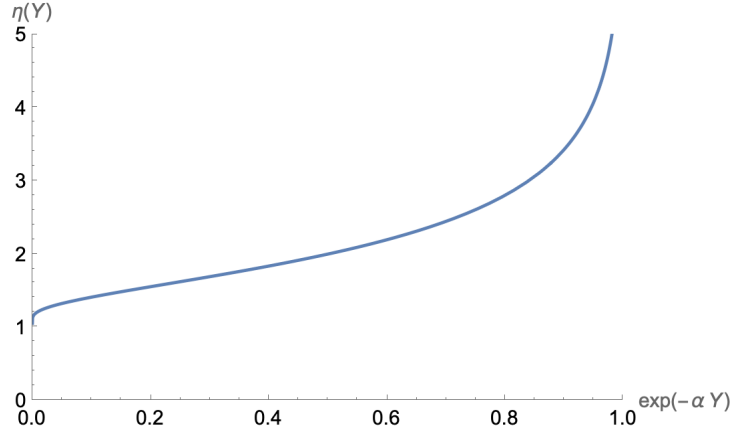


Figure 1: The uncertainty index $\eta(Y)$ derived from the probability $P_n(Y) = e^{-\alpha Y} (1 - e^{-\alpha Y})^{n-1}$ in (7) as a function of rapidity Y . The uncertainty index $\eta(Y)$ approaches unity at large rapidity indicating the maximally entangled state.

The uncertainty index $\eta(Y)$ is a very useful indicator for QCD calculations that makes it possible to use the same expression for the probability of alternative states starting at some rapidity. That would significantly simplify the involved QCD calculations.

In the next section we extend this analysis to the case of the process of different multiplicities of the produced particles using the Abramovskii-Gribov-Kancheli (AGK) cutting rules [2].

3 Entropy and AGK cutting rules

Abramovskii-Gribov-Kancheli (AGK) cutting rules [2] were originally derived to explain the relative contributions of different multiplicity of produced particles to the total cross section. The AGK paper deals with two Pomeron exchange, where one, two or none of the Pomerons can be "cut", i.e. the produced particles that build the Pomeron ladder diagrams are put "on-shell" leading to real production. The AGK cutting rules can be summarized as relative weights of the diffraction term (two uncut Pomerons), single multiplicity term (one cut and one uncut Pomeron) and the double multiplicity term (two cut Pomerons). Those weight and their signs are result of combinatorics and loop integration of the corresponding diagrams. It is important to review the origin of those weights in order to understand how to apply them to evolution equation. Fig. 2 shows a coupling of two

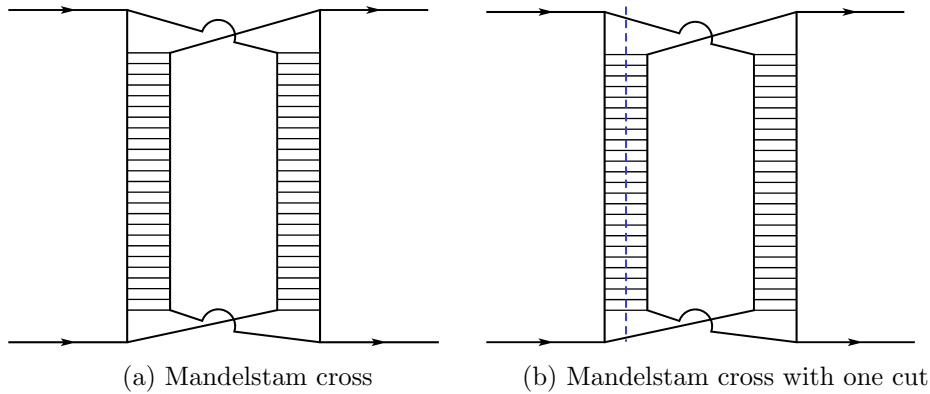


Figure 2: Two Pomeron interaction with Mandelstam cross, which allows two Pomerons to be cut simultaneously due to the non-planar cylindrical topology.

Pomerons to the target and the projectile, which is known as the Mandelstam cross. The Mandelstam cross coupling allows to put simultaneously on mass shell the intermediate produced particles in both Pomerons due to the cylindrical topology depicted in Fig. 3.

The AGK cutting rules determine the relative weights of the contribution of different multiplicity of the produced particles to the total cross section in two Pomeron exchange. Those weights are derived from combinatorics of all possible cuts and unitarity considerations, where the discontinuity of the amplitude of each cut Pomeron equals two times the imaginary part of

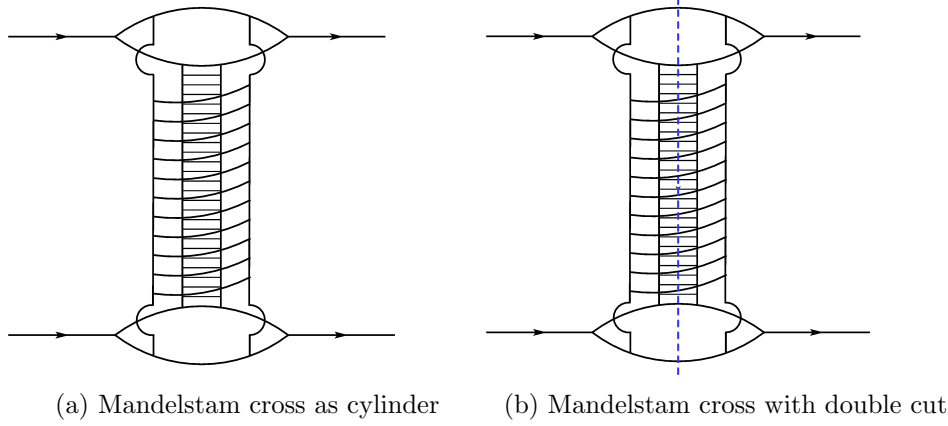


Figure 3: The cylindrical topology of two Pomeron interaction with Mandelstam cross. Two Pomerons can be simultaneously cut putting the produced particles on mass shell.

scattering amplitude of the one Pomeron exchange

$$i\delta A = i2 \operatorname{Im} A \quad (17)$$

The combinatorial coefficients, on the other hand, treat the cut and uncut Pomerons on equal basis as follows. For the contribution of diffractive cut (no cut Pomerons) the combinatorial coefficient is 2 due to two possibilities of having one or another Pomeron in the amplitude or complex conjugate amplitude as shown in Fig. 2.

The AGK cutting rules used by one of the authors [1] to extend the analysis of the dipole model in the generating function approach for zero transverse dimension [46–48]. The resulting differential equation reads

$$\begin{aligned} \frac{\partial Z(w, \bar{w}, v|Y)}{\partial Y} = & -\alpha \left\{ w(1-w) \frac{\partial Z(w, \bar{w}, v|Y)}{\partial w} + \bar{w}(1-\bar{w}) \frac{\partial Z(w, \bar{w}, v|Y)}{\partial \bar{w}} \right\} \\ & -\alpha \{ 2w\bar{w} - 2wv - 2\bar{w}v + v^2 + v \} \frac{\partial Z(w, \bar{w}, v|Y)}{\partial v} \end{aligned} \quad (18)$$

where $\alpha = \Gamma(1 \rightarrow 2)$ is the triple Pomeron vertex and the generating function is defined by

$$Z(w, \bar{w}, v|Y) = \sum_{i=0}^{\infty} \sum_{j=0}^{\infty} \sum_{k=0}^{\infty} P_{i,j,k}(Y) w^i \bar{w}^j v^k \quad (19)$$

The equation in (33) can be diagonalized in variables w , \bar{w} and $\xi = w + \bar{w} - v$ resulting in

$$\frac{\partial Z(w, \bar{w}, \xi - w - \bar{w}|Y)}{\partial Y} = \quad (20)$$

$$-\alpha \left\{ w(1-w) \frac{\partial}{\partial w} + \bar{w}(1-\bar{w}) \frac{\partial}{\partial \bar{w}} \right\} Z(w, \bar{w}, \xi - w - \bar{w}|Y) \\ -\alpha \xi(1-\xi) \frac{\partial}{\partial \xi} Z(w, \bar{w}, \xi - w - \bar{w}|Y) \quad (21)$$

The solution is a linear combination of three generating functions

$$Z(w, \bar{w}, v|Y) = \mathbf{C}_1 Z_0(w|Y) + \mathbf{C}_2 Z_0(\bar{w}|Y) + \mathbf{C}_3 Z_0(w + \bar{w} - v|Y) \quad (22)$$

where $Z_0(u|Y)$ is the solution to the simple toy model given in (6). The initial condition

$$Z(w, \bar{w}, v|Y=0) = v, \quad (23)$$

which corresponds to having one cut Pomeron at $Y=0$ implies that the solution in (34) is given by

$$Z(w, \bar{w}, v|Y) = Z_0(w|Y) + Z_0(\bar{w}|Y) - Z_0(w + \bar{w} - v|Y). \quad (24)$$

The generating function in (24) solves the differential equation in (33) and can be used for deriving scattering amplitude for various processes. However, it follows directly from the definition of the generating function and the relative signs of different AGK terms in the differential equation in (33) that in some cases the expression in (24) leads to negative probabilities, which are perfectly allowed in Quantum Field Theory, where the AGK cutting rules were derived. Any attempt of using the QFT results directly in Quantum Mechanics would fail due to the presence of the negative probabilities that have no proper interpretation in Quantum Mechanics. One of such applications is the use of the concept of von Neumann entropy which requires, by definition, all probabilities to be positive definite. The von Neumann entropy is defined by

$$S = -\text{Tr}(\rho \ln \rho), \quad (25)$$

where the probability density matrix

$$\rho = \sum_j p_j |j\rangle \langle j|. \quad (26)$$

Plugging ρ into the definition in (25) one obtains

$$S = - \sum_j p_j \ln p_j. \quad (27)$$

This definition of the entropy implies the well defined space of states $\langle j|$ and the positiveness of p_j . None of those conditions is fulfilled in QFT.

Nevertheless, it is still possible to apply AGK cutting rules in the modified version for the entanglement analysis using von Neumann entropy. The first step is to understand the origin of the coefficients of different multiplicity terms, σ_n that lead to the AGK coefficients

$$\sigma_0 \div \sigma_1 \div \sigma_2 = 2 \div (-8) \div 4 \quad (28)$$

that sum to the total cross section

$$\sigma_0 + \sigma_1 + \sigma_2 = -2\text{Im}A_1\text{Im}A_2 \quad (29)$$

Those relative weight coefficients are obtained from *a*) positive definite combinatorial weights of different ways to cut two Pomerons *b*) a minus sign that appears every time the Pomeron is cut. It is worth emphasizing the latter. The leading contribution of the cut Pomeron is given by

$$i\delta A = i2\text{Im}A, \quad (30)$$

that can be derived by the loop integration with the produces particles put on-shell, in contrast to the uncut Pomeron where the integration is performed calculating the residue at one of the poles of the loop integration over longitudinal momentum. This is the case in the Minkowski space, where the longitudinal component of the loop momentum comes with a minus sign with respect to the transverse components. On contrary, in the Euclidean space all momenta components come at the equal basis and thus the relative sign between the cut Pomeron and the uncut Pomeron contributions does not appear resulting in the AGK weights in the Euclidean space

$$\sigma_0^{\text{Euclidean}} \div \sigma_1^{\text{Euclidean}} \div \sigma_2^{\text{Euclidean}} = 2 \div 8 \div 4 \quad (31)$$

The immediate question that emerges in this context is if the positive definite AGK weights in the Euclidean space can sum into a meaningful expression that can be associated with the total cross section of the two Pomeron exchange, similar to the Minkowski space where the expression in (29) holds.

In the Euclidean space the sums of all contributions of the different multiplicity in (31) gives

$$\sigma_0^{\text{Euclidean}} + \sigma_1^{\text{Euclidean}} + \sigma_2^{\text{Euclidean}} = 10\text{Im}A_1\text{Im}A_2 \quad (32)$$

and there is no analytic continuation from the Euclidean to the Minkowski space that would give the physical total cross section in (29). This question has been well studied in the context of the helicity amplitudes [52–57] and it was shown that the operation of the analytic continuation from the Euclidean to the Minkowski space does not commute with the operation of taking Regge limit, i.e. considering the multi-Regge kinematics. This non interchangeability of analityc continuation and the Regge limit is not relevant in the context of the entropy and the entanglement because the statistics of different multiplicities contributions is correctly represented by counting the number of cut Pomerons and uncut Pomerons with positive definite AGK weights in the Euclidean space in (31).

In other words, it is perfectly possible to use the modified AGK weights in the Euclidean space in (31) to count number of cut and uncut Pomerons, but it is not possible to directly apply them to calculation of the total cross section due to non-interchangeability of the operation of taking Regge limit the operation of the analytic continuation from the Euclidean space to the Minkowski space. The differential evolution equation based on the AGK weights in (33) should be modified in the Euclidean space as follows

$$\begin{aligned} \frac{\partial Z^{\text{Eucl}}(w, \bar{w}, v|Y)}{\partial Y} = & \\ -\alpha \left\{ w(1-w) \frac{\partial Z^{\text{Eucl}}(w, \bar{w}, v|Y)}{\partial w} + \bar{w}(1-\bar{w}) \frac{\partial Z^{\text{Eucl}}(w, \bar{w}, v|Y)}{\partial \bar{w}} \right\} & \\ +\alpha \left\{ 2w\bar{w} + 2wv + 2\bar{w}v + v^2 - v \right\} \frac{\partial Z^{\text{Eucl}}(w, \bar{w}, v|Y)}{\partial v} & \end{aligned} \quad (33)$$

which is solved by

$$Z^{\text{Eucl}}(w, \bar{w}, v|Y) = \mathbb{C}_1 Z_0(w|Y) + \mathbb{C}_2 Z_0(\bar{w}|Y) + \mathbb{C}_3 Z_0(w + \bar{w} + v|Y) \quad (34)$$

where $Z_0(u|Y)$ is the solution to the simple toy model (see (6))

$$Z_0(u|Y) = \frac{ue^{-\alpha Y}}{1 + u(e^{-\alpha Y} - 1)}. \quad (35)$$

In this paper we discuss a process where there is at least one cut Pomeron. In this case, the only relevant terms in (34) is the term that depends on v ,

namely, $Z_0(v + w + \bar{w}|Y)$. Using the definition of the generating function

$$\begin{aligned} Z_0(v + w + \bar{w}|Y) &= \sum_{i,j,k=0}^{\infty} P_{i,j,k}(Y) v^i w^j \bar{w}^k 3^{i+j+k} (1 - \delta_{i,0} \delta_{j,0} \delta_{k,0}) \quad (36) \\ &= \frac{v + w + \bar{w}}{v + w + \bar{w} + (1 - v - w - \bar{w})e^{\alpha Y}} \end{aligned}$$

we extract the probability

$$P_{i,j,k}(Y) = \frac{1}{3^{i+j+k}} \frac{(i+j+k)!}{i! j! k!} e^{-\alpha Y} (1 - e^{-\alpha Y})^{i+j+k-1} \quad (37)$$

Note the 3^{i+j+k} term in (37) introduced as a proper normalization due to the fact that the argument $w + \bar{w} + v$ equals 3 at $w = \bar{w} = v = 1$ in contrast to the definition of $Z_0(u|Y)$ in (1). The first two terms in (34) are not relevant for extracting the probability for having at least one cut Pomeron as they do not make any contribution to the cut Pomerons.

The probability $P_{i,j,k}$ is symmetrical with respect to all its indices and its represent a probability of finding i cut Pomerons, j uncut Pomerons in the amplitude and k uncut Pomerons in the complex conjugate amplitude at any given rapidity Y .

We are interested in a case, where one has at least one cut Pomeron at any given rapidity Y limiting the total number of Pomerons to $m = i + j + k$.

We define the probability P_m of having m Pomerons of any kind under condition that at least one of them is the cut Pomeron, i.e.

$$P_m(Y) = \sum_{i=1}^m \sum_{j=0}^{m-i} \sum_{k=0}^{m-i-j} P_{i,j,k}(Y) \quad (38)$$

it reads

$$\begin{aligned} P_m(Y) &= e^{-\alpha Y} (1 - e^{-\alpha Y})^{m-1} \frac{m!}{3^m} \sum_{i=1}^m \sum_{j=0}^{m-i} \frac{1}{i! j! (m-i-j)!} \quad (39) \\ &= e^{-\alpha Y} (1 - e^{-\alpha Y})^{m-1} \frac{m!}{3^m} \sum_{i=1}^m \frac{2^{m-i}}{i! (m-i)! 3^m} \end{aligned}$$

leading to

$$P_m(Y) = \left(1 - \frac{2^m}{3^m}\right) e^{-\alpha Y} (1 - e^{-\alpha Y})^{m-1}$$

Note that $P_m(Y)$ does not account for cases of having only m uncut Pomerons and thus the sum $\sum_{m=1}^{\infty} P_m(Y)$ is not strictly equal to unity, i.e.

$$\sum_{m=1}^{\infty} P_m(Y) = \frac{1}{1 + 2e^{-\alpha Y}} \quad (40)$$

which goes to unity when $Y \rightarrow \infty$ because the contribution of those states at large rapidity is negligible. According to the boundary condition of having at least one cut Pomeron at any rapidity we exclude those states normalizing $P_m(Y)$ as follows

$$\tilde{P}_m(Y) = \frac{P_m(Y)}{\sum_{m=1}^{\infty} P_m(Y)} \quad (41)$$

resulting in

$$\tilde{P}_m(Y) = \left(1 - \frac{2^m}{3^m}\right) e^{-\alpha Y} (1 - e^{-\alpha Y})^{m-1} (1 + 2e^{-\alpha Y}) \quad (42)$$

The normalized probability $\tilde{P}_m(Y)$ sums to unity

$$\sum_{m=1}^{\infty} \tilde{P}_m(Y) = 1 \quad (43)$$

and satisfies the initial condition

$$\tilde{P}_m(Y=0) = \delta_{m,1}. \quad (44)$$

This should be compared to the probability used by Kharzeev and Levin (the KL model) [3]

$$P_m^{KL}(Y) = e^{-\alpha Y} (1 - e^{-\alpha Y})^{m-1} \quad (45)$$

used for calculating the entropy and moments C_q for comparison to the experimental data. We follow the lines of the KL paper [3] as well as the more recent works [4–17] and calculate the experimental observables using the probability $\tilde{P}_m(Y)$ in (42) based on the AGK cutting rules. The mean multiplicity of produced particles corresponds the mean number of Pomerons that is given by

$$\langle m \rangle = \sum_{m=1}^{\infty} m \tilde{P}_m(Y) = e^{\alpha Y} - 1 + \frac{3}{1 + 2e^{-\alpha Y}}, \quad (46)$$

and at large rapidity takes form

$$\langle m \rangle \simeq e^{\alpha Y} + 2 - 6e^{-\alpha Y}. \quad (47)$$

The entropy is defined as

$$S = - \sum_{m=1}^{\infty} \tilde{P}_m(Y) \ln \tilde{P}_m(Y) \quad (48)$$

and can be reasonably approximated and found analytically using

$$\log \left(1 - \frac{2^m}{3^m} \right) = - \sum_{k=1}^{\infty} \left(\frac{2^m}{3^m} \right)^k, \quad (49)$$

where we limit ourselves to the first hundred terms. Plugging this in (48) for large rapidity we obtain the first three leading terms of the entropy at high energies

$$S = - \sum_{m=1}^{\infty} \tilde{P}_m(Y) \ln \tilde{P}_m(Y) \simeq \alpha Y + 1 - e^{-\alpha Y} \quad (50)$$

At $Y = 0$ the entropy vanishes due to the fact that $\tilde{P}_m(Y = 0) = \delta_{m,1}$. Vanishing entropy at $Y = 0$ implies that the system is in the pure state and thus it is maximally ordered. On the other hand, at large rapidity the entropy grows as the mean number of Pomerons

$$S \simeq \alpha Y \simeq \ln \langle m \rangle \quad (51)$$

implying maximally entangled state. The entropy of the Kharzeev-Levin model has the form

$$S_{KL} = \alpha Y - e^{\alpha Y} (1 - e^{-\alpha Y}) \log (1 - e^{-\alpha Y}) \simeq \alpha Y + 1 - \frac{e^{-\alpha Y}}{2} \quad (52)$$

leading to the same asymptotics

$$S_{KL} \simeq \alpha Y \simeq \ln \langle m \rangle \quad (53)$$

The uncertainty index $\eta(Y)$ defined in (14) is also of the similar behaviour for the two models as one can see from their comparison in Fig. 4.

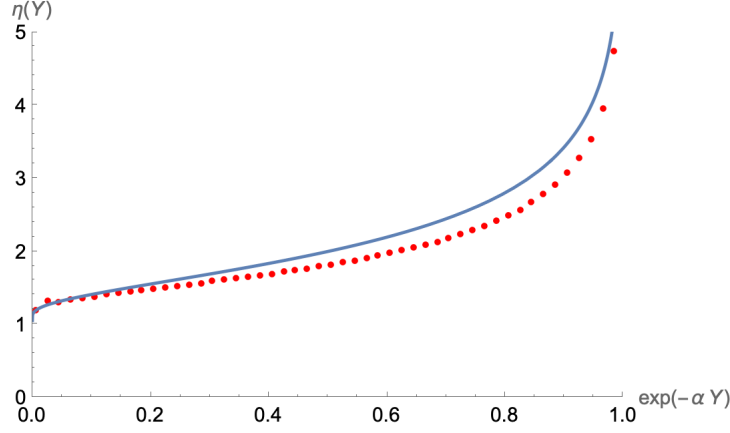


Figure 4: Comparison of the uncertainty index $\eta(Y)$ derived from the probability in Kharzeev-Levin model (solid line) and our model (the AGK model) (red dotted line). The uncertainty index $\eta(Y)$ approaches unity at large rapidity indicating the maximally entangled state.

4 Comparison to Experimental Data

In the framework of the Koba-Nielsen-Olesen (KNO) [45] scaling analysis, it is assumed that at high energies the probability of having n Pomerons should scale as

$$P_n(Y) = \frac{1}{\langle n \rangle} \Psi \left(\frac{n}{\langle n \rangle} \right), \quad (54)$$

where $\Psi(x)$ is a smooth bounded analytic function and $\langle n \rangle$ is the average multiplicity of the produced particles. If the KNO scaling holds the q -moments C_q are defined by

$$C_q = \frac{\langle n^q \rangle}{\langle n \rangle^q}, \quad (55)$$

should be energy independent, because

$$\langle n^q \rangle = \sum_{n=1}^{\infty} n^q P_n(y) \quad (56)$$

can be approximated by the integral

$$\langle n^q \rangle = \int \frac{n^q}{\langle n \rangle} \Psi \left(\frac{n}{\langle n \rangle} \right) dn = \langle n \rangle^q \text{Const}_q \quad (57)$$

where Const_q is some number, which does not depend on energy. All energy dependence is scaled in $\langle n \rangle^q$ and in accordance to the definition of the moments C_q it cancels with the denominator provided the KNO scaling holds, namely plugging (57) into (55) we obtain

$$C_q = \frac{\langle n^q \rangle}{\langle n \rangle^q} = \frac{\langle n \rangle^q \text{Const}_q}{\langle n \rangle^q} = \text{Const}_q. \quad (58)$$

This implies that the moments C_q are independent of energy within limits of the KNO scaling conditions.

In order to check the validity of our model we calculate the moments C_q using the AGK based probability in (42) and compare it to the experimental data. The probability calculated in our model using the AGK cutting rules in (42) is given by

$$\tilde{P}_n(x) = \left(1 - \frac{2^n}{3^n}\right) x(1-x)^{n-1}(1+2x) \quad (59)$$

where $x = e^{-\alpha Y}$.

The average number of Pomerons for the AGK probability reads

$$\langle n^q \rangle|_{q=1} = \langle n \rangle = \frac{3}{2x+1} + \frac{1}{x} - 1 \quad (60)$$

In the general case of natural q the numerator in (55) can be written as follows

$$\langle n^q \rangle = \frac{x(1+2x)}{1-x} \left[\text{Li}_{-q}(1-x) - \text{Li}_{-q}\left(\frac{2(1-x)}{3}\right) \right], \quad (61)$$

where $x = e^{-\alpha Y}$ and $\text{Li}_b(z)$ is the special function named polylog function (polylogarithm), which cannot be expressed in terms of the elementary functions for positive integer values of $b > 1$. For the negative integer index b it is a rational function given by

$$\text{Li}_{-q}(z) = \left(z \frac{\partial}{\partial z} \right)^q \frac{z}{1-z}, \quad q = 1, 2, 3... \quad (62)$$

The first few polylogarithms of the negative integer index read

$$\begin{aligned}
\text{Li}_{-1}(z) &= \frac{z}{(1-z)^2}, \\
\text{Li}_{-2}(z) &= \frac{z^2 + z}{(1-z)^3}, \\
\text{Li}_{-3}(z) &= \frac{z^3 + 4z^2 + z}{(1-z)^4}, \\
\text{Li}_{-4}(z) &= \frac{z^4 + 11z^3 + 11z^2 + z}{(1-z)^5}, \\
\text{Li}_{-5}(z) &= \frac{z^5 + 26z^4 + 66z^3 + 26z^2 + z}{(1-z)^6}
\end{aligned} \tag{63}$$

Plugging (61) and (60) into (55) we obtain

$$C_q = \frac{\langle n^q \rangle}{\langle n \rangle^q} = \frac{x^{q+1}(1+2x)^{q+1}}{(1-x)(1+4x-2x^2)} \left[\text{Li}_{-q}(1-x) - \text{Li}_{-q}\left(\frac{2(1-x)}{3}\right) \right] \tag{64}$$

Note that the expression $1+4x-2x^2$ never turns zero as follows from the definition $x = e^{-\alpha Y}$. The divergent overall factor $1/(1-x)$ is cancelled by highly convergent difference of the polylog functions in the brackets in (64). The first five moments C_q read

$$\begin{aligned}
C_2 &= \frac{4x^4 - 26x^3 + 18x^2 + 11x + 2}{(2x^2 - 4x - 1)^2}, \\
C_3 &= \frac{4x^4 - 56x^3 + 37x^2 + 18x + 6}{(2x^2 - 4x - 1)^2}, \\
C_4 &= \frac{16x^8 - 568x^7 + 2804x^6 - 3222x^5 - 410x^4 + 619x^3 + 614x^2 + 204x + 24}{(2x^2 - 4x - 1)^4}, \\
C_5 &= \frac{16x^8 - 1168x^7 + 8664x^6 - 10732x^5 - 59x^4 + 690x^3 + 1830x^2 + 720x + 120}{(2x^2 - 4x - 1)^4}
\end{aligned} \tag{65}$$

or in terms of the average number of Pomerons $\langle n \rangle$ in (60)

$$\begin{aligned}
C_2 &= \frac{24 + 2\langle n \rangle^2 - 5\sqrt{\langle n \rangle^2 + 24}}{\langle n \rangle^2}, \\
C_3 &= \frac{145 + 6\langle n \rangle^2 - 30\sqrt{\langle n \rangle^2 + 24}}{\langle n \rangle^2}, \\
C_4 &= \frac{7080 + 1022\langle n \rangle^2 + 24\langle n \rangle^4 - 5(36\langle n \rangle^2 + 289)\sqrt{\langle n \rangle^2 + 24}}{\langle n \rangle^4}, \\
C_5 &= \frac{106561 + 8070\langle n \rangle^2 + 120\langle n \rangle^4 - 150(8\langle n \rangle^2 + 145)\sqrt{\langle n \rangle^2 + 24}}{\langle n \rangle^4}
\end{aligned} \tag{66}$$

The moments C_q in (67) are expressed in terms of the multiplicity $\langle n \rangle$ directly available in the experimental data without any adjustable parameter. This fact allows a self-consistent direct comparison to the experimental data. We compare our results to the $\mathbf{p} - \mathbf{p}$ data by ALICE Collaboration (see Table 13 in [49]). The experimental data is given for three pseudorapidity windows $\Delta\eta = 0$, $\Delta\eta = 1$ and $\Delta\eta = 1.5$. From the definition of the pseudorapidity it follows that for our model formulated in zero transverse dimension the pseudorapidity should go to infinity meaning the detector performs the measurement in the entire solid angle of 4π . Thus the appropriate available set of the experimental data for testing our model is for $\Delta\eta = 1.5$.

In Table 1 we compare the moments C_q calculated using our model (AGK model) and the Kharzeev-Levin model [3] (KL model) to the experimental data for the $\mathbf{p} - \mathbf{p}$ collisions by ALICE Collaboration (see Table 13 in [49]). As we have already mentioned, the comparison to the experimental data is done without any adjustable parameter in both models, which makes it possible to compare two different models in the self-consistent way. It is clearly seen from the direct comparison to the experimental data in Table 1 that our model based on AGK cutting rules performs significantly better than the KL model in a broad range of the center-of-mass energy.

The main results of this section are given in the attached **Mathematica** file.

$\sqrt{s} = 0.9 \text{ TeV}$			
observable	experiment	AGK model	KL model
$\langle n \rangle$	11.8 ± 0.4	11.8 ± 0.4	11.8 ± 0.4
C_2	1.7 ± 0.1	1.71 ± 0.01	1.92 ± 0.03
C_3	3.9 ± 0.3	4.29 ± 0.04	5.50 ± 0.02
C_4	11 ± 1	14.2 ± 0.2	21.1 ± 0.1
C_5	36 ± 6	59.0 ± 1.1	100.7 ± 0.6
$\sqrt{s} = 2.76 \text{ TeV}$			
observable	experiment	AGK model	KL model
$\langle n \rangle$	14.2 ± 0.7	14.2 ± 0.7	14.2 ± 0.7
C_2	1.8 ± 0.1	1.75 ± 0.01	1.93 ± 0.01
C_3	4.5 ± 0.6	4.48 ± 0.05	5.58 ± 0.02
C_4	14 ± 3	15.3 ± 0.3	21.5 ± 0.1
C_5	51 ± 13	65.2 ± 1.6	103.8 ± 0.8
$\sqrt{s} = 7 \text{ TeV}$			
observable	experiment	AGK model	KL model
$\langle n \rangle$	17.5 ± 0.6	17.5 ± 0.6	17.5 ± 0.6
C_2	1.9 ± 0.1	1.78 ± 0.01	1.94 ± 0.01
C_3	5.0 ± 0.4	4.69 ± 0.03	5.66 ± 0.01
C_4	16 ± 2	16.5 ± 0.2	21.99 ± 0.07
C_5	64 ± 11	72.1 ± 1.1	106.8 ± 0.4
$\sqrt{s} = 8 \text{ TeV}$			
observable	experiment	AGK model	KL model
$\langle n \rangle$	17.8 ± 1.1	17.8 ± 1.1	17.8 ± 1.1
C_2	1.9 ± 0.1	1.78 ± 0.01	1.94 ± 0.01
C_3	5.2 ± 0.8	4.71 ± 0.06	5.67 ± 0.02
C_4	18 ± 4	16.5 ± 0.3	22.02 ± 0.12
C_5	70 ± 20	72.6 ± 2.0	107.0 ± 0.5

Table 1: Comparison of the q -moments C_q of our model (AGK model) and Kharzeev-Levin model (KL model) to the experimental data for the $\text{p} - \text{p}$ collision by ALICE Collaboration (see Table 13 in [49]). Here we consider the pseudorapidity $\eta = 1.5$ and the center-of-mass energies $\sqrt{s} = 0.9 \text{ TeV}$, $\sqrt{s} = 2.76 \text{ TeV}$, $\sqrt{s} = 7 \text{ TeV}$ and $\sqrt{s} = 8 \text{ TeV}$. Note that we use as the input the experimental value of the mean multiplicity $\langle n \rangle$ so that the AGK model and the KL model have no freedom in adjusting any free parameter such as α_s or Y_0 . Our model (AGK model) consistently better than the KL model in describing the experimental data in the wide range of energies.

5 Conclusion and Discussions

In this paper we analysed the Pomeron evolution based on the AGK cutting rules. A direct application of the AGK rules to the evolution equation leads to negative probabilities that follow from negative AGK weights derived in the Minkowski space. We reformulate the Pomeron evolution in the Euclidean space using the combinatorial coefficients derived in the original AGK paper. The resulting positive definite probabilities in (37) and (42) for cut and uncut Pomerons are then used in calculating the von Neumann entropy and the q -moments C_q as a function of rapidity (66) and a function of the mean multiplicity of the produced particles in (67). The latter is shown to successfully describe the experimental data for $\mathbf{p} - \mathbf{p}$ collision by ALICE Collaboration without any free adjustable parameter (see Table 1). We also show that our model based on AGK cutting rules performs consistently better than the KL model in describing the experimental data in the wide range of energies.

The main results of this study are given in the attached `Mathematica` file.

6 Acknowledgements

We are indebted to Sergey Bondarenko for inspiring discussions on the topic. This research is supported in part by the Council of Higher Education of Israel through the grant "Support program of the High Energy Physics".

References

- [1] E. Levin and A. Prygarin, “Inclusive gluon production in the dipole approach: AGK cutting rules,” *Phys. Rev. C* **78**, 065202 (2008) doi:10.1103/PhysRevC.78.065202 [arXiv:0804.4747 [hep-ph]].
- [2] V. A. Abramovsky, V. N. Gribov and O. V. Kancheli, “Character of Inclusive Spectra and Fluctuations Produced in Inelastic Processes by Multi - Pomeron Exchange,” *Yad. Fiz.* **18**, 595-616 (1973)
- [3] D. E. Kharzeev and E. M. Levin, “Deep inelastic scattering as a probe of entanglement,” *Phys. Rev. D* **95**, no.11, 114008 (2017) doi:10.1103/PhysRevD.95.114008 [arXiv:1702.03489 [hep-ph]].
- [4] D. E. Kharzeev and E. Levin, “Deep inelastic scattering as a probe of entanglement: Confronting experimental data,” *Phys. Rev. D* **104**, no.3, L031503 (2021) doi:10.1103/PhysRevD.104.L031503 [arXiv:2102.09773 [hep-ph]].
- [5] K. Zhang, K. Hao, D. Kharzeev and V. Korepin, “Entanglement entropy production in deep inelastic scattering,” *Phys. Rev. D* **105**, no.1, 014002 (2022) doi:10.1103/PhysRevD.105.014002 [arXiv:2110.04881 [quant-ph]].
- [6] A. Florio, D. Frenklakh, K. Ikeda, D. Kharzeev, V. Korepin, S. Shi and K. Yu, “Real-Time Nonperturbative Dynamics of Jet Production in Schwinger Model: Quantum Entanglement and Vacuum Modification,” *Phys. Rev. Lett.* **131**, no.2, 021902 (2023) doi:10.1103/PhysRevLett.131.021902 [arXiv:2301.11991 [hep-ph]].
- [7] M. Hentschinski, D. E. Kharzeev, K. Kutak and Z. Tu, *Phys. Rev. Lett.* **131**, no.24, 241901 (2023) doi:10.1103/PhysRevLett.131.241901 [arXiv:2305.03069 [hep-ph]].
- [8] M. Hentschinski, “Entanglement entropy in high energy collisions of electrons and protons,” *Rev. Mex. Fis. Suppl.* **4**, no.2, 021110 (2023) doi:10.31349/SuplRevMexFis.4.021110
- [9] K. Kutak, “Entanglement entropy of proton and its relation to thermodynamics entropy,” [arXiv:2310.18510 [hep-ph]].
- [10] K. Kutak, “Entanglement Entropy and Proton’s Structure,” *Acta Phys. Polon. Supp.* **17**, no.2, 2-A3 (2024) doi:10.5506/APhysPolBSupp.17.2-A3

- [11] K. Kutak, “Entanglement Entropy, Krylov Complexity, and DIS Data,” *Acta Phys. Polon. Supp.* **18**, no.5, 5-A4 (2025) doi:10.5506/APhysPolBSupp.18.5-A4
- [12] L. S. Moriggi, G. S. Ramos and M. V. T. Machado, “Multiplicity dependence of the pT-spectra for identified particles and its relationship with partonic entropy,” *Phys. Rev. D* **110**, no.3, 034005 (2024) doi:10.1103/PhysRevD.110.034005 [arXiv:2405.01712 [hep-ph]].
- [13] P. Caputa and K. Kutak, “Krylov complexity and gluon cascades in the high energy limit,” *Phys. Rev. D* **110**, no.8, 085011 (2024) doi:10.1103/PhysRevD.110.085011 [arXiv:2404.07657 [hep-ph]].
- [14] S. Bhattacharya, R. Boussarie and Y. Hatta, “Spin-orbit entanglement in the Color Glass Condensate,” *Phys. Lett. B* **859**, 139134 (2024) doi:10.1016/j.physletb.2024.139134 [arXiv:2404.04208 [hep-ph]].
- [15] Y. Liu, M. A. Nowak and I. Zahed, “Mueller’s dipole wave function in QCD: Emergent Koba-Nielsen-Olesen scaling in the double logarithm limit,” *Phys. Rev. D* **108**, no.3, 034017 (2023) doi:10.1103/PhysRevD.108.034017 [arXiv:2211.05169 [hep-ph]].
- [16] Y. Hatta and J. Montgomery, “Maximally entangled gluons for any x ,” *Phys. Rev. D* **111**, no.1, 014024 (2025) doi:10.1103/PhysRevD.111.014024 [arXiv:2410.16082 [hep-ph]].
- [17] E. Levin, “Particle production in a toy model: Multiplicity distribution and entropy,” *Phys. Rev. D* **111**, no.1, 016019 (2025) doi:10.1103/PhysRevD.111.016019 [arXiv:2412.02504 [hep-ph]].
- [18] A. Kovner, M. Lublinsky and M. Serino, “Entanglement entropy, entropy production and time evolution in high energy QCD,” *Phys. Lett. B* **792**, 4-15 (2019) doi:10.1016/j.physletb.2018.10.043 [arXiv:1806.01089 [hep-ph]].
- [19] N. Armesto, F. Dominguez, A. Kovner, M. Lublinsky and V. Skokov, “The Color Glass Condensate density matrix: Lindblad evolution, entanglement entropy and Wigner functional,” *JHEP* **05**, 025 (2019) doi:10.1007/JHEP05(2019)025 [arXiv:1901.08080 [hep-ph]].
- [20] R. Peschanski and S. Seki, “Evaluation of Entanglement Entropy in High Energy Elastic Scattering,” *Phys. Rev. D* **100**, no.7, 076012 (2019) doi:10.1103/PhysRevD.100.076012 [arXiv:1906.09696 [hep-th]].

- [21] G. S. Ramos and M. V. T. Machado, “Investigating entanglement entropy at small- x in DIS off protons and nuclei,” *Phys. Rev. D* **101**, no.7, 074040 (2020) doi:10.1103/PhysRevD.101.074040 [arXiv:2003.05008 [hep-ph]].
- [22] Y. Afik and J. R. M. de Nova, “Quantum information with top quarks in QCD,” *Quantum* **6**, 820 (2022) doi:10.22331/q-2022-09-29-820 [arXiv:2203.05582 [quant-ph]].
- [23] G. S. Ramos and M. V. T. Machado, “Investigating the QCD dynamical entropy in high-energy hadronic collisions,” *Phys. Rev. D* **105**, no.9, 094009 (2022) doi:10.1103/PhysRevD.105.094009 [arXiv:2203.10986 [hep-ph]].
- [24] H. Duan, A. Kovner and V. V. Skokov, “Classical entanglement and entropy,” *Int. J. Mod. Phys. A* **39**, no.29, 2450104 (2024) doi:10.1142/S0217751X24501045 [arXiv:2301.05735 [quant-ph]].
- [25] A. Dumitru, A. Kovner and V. V. Skokov, “Entanglement entropy of the proton in coordinate space,” *Phys. Rev. D* **108**, no.1, 014014 (2023) doi:10.1103/PhysRevD.108.014014 [arXiv:2304.08564 [hep-ph]].
- [26] H. G. Dosch, G. F. de Teramond and S. J. Brodsky, “Entropy from entangled parton states and high-energy scattering behavior,” *Phys. Lett. B* **850**, 138521 (2024) doi:10.1016/j.physletb.2024.138521 [arXiv:2304.14207 [hep-ph]].
- [27] A. Hutson and R. Bellwied, “Exploring Particle Production and Thermal-Like Behavior through Quantum Entanglement,” [arXiv:2410.17429 [hep-ph]].
- [28] L. S. Moriggi and M. V. T. Machado, “Precise determination of the Pomeron intercept via a scaling entropy analysis,” *Phys. Rev. D* **111**, no.1, 014017 (2025) doi:10.1103/PhysRevD.111.014017 [arXiv:2412.16348 [hep-ph]].
- [29] G. S. Ramos, “Investigating Notions of Entropy and Its Production in High Energy Particle Collisions,” [arXiv:2502.01038 [hep-ph]].
- [30] W. Qi, Z. Guo and B. W. Xiao, “Studying Maximal Entanglement and Bell Nonlocality at an Electron-Ion Collider,” [arXiv:2506.12889 [hep-ph]].

- [31] G. S. Ramos, L. S. Moriggi and M. V. T. Machado, “Investigating QCD dynamical entropy in high-energy nuclear collisions,” *Phys. Lett. B* **868**, 139737 (2025) doi:10.1016/j.physletb.2025.139737 [arXiv:2507.09349 [hep-ph]].
- [32] K. A. Mamo, “Entanglement, Trace Anomaly and Confinement in QCD,” [arXiv:2507.00176 [hep-ph]].
- [33] H. Duan, C. Akkaya, A. Kovner and V. V. Skokov, “Entanglement, partial set of measurements, and diagonality of the density matrix in the parton model,” *Phys. Rev. D* **101**, no.3, 036017 (2020) doi:10.1103/PhysRevD.101.036017 [arXiv:2001.01726 [hep-ph]].
- [34] A. Baty, P. Gardner and W. Li, “Novel observables for exploring QCD collective evolution and quantum entanglement within individual jets,” *Phys. Rev. C* **107**, no.6, 064908 (2023) doi:10.1103/PhysRevC.107.064908 [arXiv:2104.11735 [hep-ph]].
- [35] A. Florio and D. E. Kharzeev, “Gibbs entropy from entanglement in electric quenches,” *Phys. Rev. D* **104**, no.5, 056021 (2021) doi:10.1103/PhysRevD.104.056021 [arXiv:2106.00838 [hep-th]].
- [36] S. Griener, D. E. Kharzeev and I. Zahed, “Entanglement in a holographic Schwinger pair with confinement,” *Phys. Rev. D* **108**, no.8, 086030 (2023) doi:10.1103/PhysRevD.108.086030 [arXiv:2305.07121 [hep-th]].
- [37] G. A. Miller, “Entanglement of elastic and inelastic scattering,” *Phys. Rev. C* **108**, no.4, L041601 (2023) doi:10.1103/PhysRevC.108.L041601 [arXiv:2306.14800 [nucl-th]].
- [38] U. Gürsoy, D. E. Kharzeev and J. F. Pedraza, “Universal rapidity scaling of entanglement entropy inside hadrons from conformal invariance,” *Phys. Rev. D* **110**, no.7, 074008 (2024) doi:10.1103/PhysRevD.110.074008 [arXiv:2306.16145 [hep-th]].
- [39] J. Barata, W. Gong and R. Venugopalan, “Realtime dynamics of hyperon spin correlations from string fragmentation in a deformed four-flavor Schwinger model,” *Phys. Rev. D* **109**, no.11, 116003 (2024) doi:10.1103/PhysRevD.109.116003 [arXiv:2308.13596 [hep-ph]].
- [40] S. Griener, K. Ikeda, D. E. Kharzeev and I. Zahed, “Entanglement in massive Schwinger model at finite temperature and density,” *Phys.*

- Rev. D **109**, no.1, 016023 (2024) doi:10.1103/PhysRevD.109.016023 [arXiv:2312.03172 [hep-th]].
- [41] B. J. J. Khor, D. M. Kurkcuoglu, T. J. Hobbs, G. N. Perdue and I. Klich, “Confinement and Kink Entanglement Asymmetry on a Quantum Ising Chain,” Quantum **8**, 1462 (2024) doi:10.22331/q-2024-09-06-1462 [arXiv:2312.08601 [quant-ph]].
 - [42] A. Florio, “Two-fermion negativity and confinement in the Schwinger model,” Phys. Rev. D **109**, no.7, L071501 (2024) doi:10.1103/PhysRevD.109.L071501 [arXiv:2312.05298 [hep-th]].
 - [43] A. J. Barr, M. Fabbrichesi, R. Floreanini, E. Gabrielli and L. Marzola, “Quantum entanglement and Bell inequality violation at colliders,” Prog. Part. Nucl. Phys. **139**, 104134 (2024) doi:10.1016/j.pnpnp.2024.104134 [arXiv:2402.07972 [hep-ph]].
 - [44] Y. Meurice, “Lower bounds on entanglement entropy without twin copy,” Phys. Rev. Res. **7**, no.2, L022023 (2025) doi:10.1103/PhysRevResearch.7.L022023 [arXiv:2404.09935 [quant-ph]].
 - [45] Z. Koba, H. B. Nielsen and P. Olesen, “Scaling of multiplicity distributions in high-energy hadron collisions,” Nucl. Phys. B **40**, 317-334 (1972) doi:10.1016/0550-3213(72)90551-2
 - [46] E. Levin and A. Prygarin, “The BFKL Pomeron Calculus in zero transverse dimension: Summation of the Pomeron loops and the generating functional for the multiparticle production processes,” Eur. Phys. J. C **53**, 385-399 (2008) doi:10.1140/epjc/s10052-007-0458-5 [arXiv:hep-ph/0701178 [hep-ph]].
 - [47] M. Kozlov, E. Levin and A. Prygarin, “The BFKL Pomeron calculus in the dipole approach,” Nucl. Phys. A **792**, 122-151 (2007) doi:10.1016/j.nuclphysa.2007.05.008 [arXiv:0704.2124 [hep-ph]].
 - [48] A. Kormilitzin, E. Levin and A. Prygarin, “Multiparticle production in the mean field approximation of high density QCD,” Nucl. Phys. A **813**, 1-13 (2008) doi:10.1016/j.nuclphysa.2008.09.006 [arXiv:0807.3413 [hep-ph]].
 - [49] J. Adam *et al.* [ALICE], “Charged-particle multiplicities in proton-proton collisions at $\sqrt{s} = 0.9$ to 8 TeV,” Eur. Phys. J. C **77**,

- no.1, 33 (2017) doi:10.1140/epjc/s10052-016-4571-1 [arXiv:1509.07541 [nucl-ex]].
- [50] A. R. Wilcoxon, "Indices of qualitative variation" (1967), <https://www.osti.gov/servlets/purl/4167340>
 - [51] N. Johnson, A. Kemp, S. Kotz "Univariate Discrete Distributions", Wiley Series in Probability and Statistics (1 ed.). Wiley. doi:10.1002/0471715816. ISBN 978-0-471-27246-5
 - [52] J. Bartels, L. N. Lipatov and A. Sabio Vera, "N=4 supersymmetric Yang Mills scattering amplitudes at high energies: The Regge cut contribution," Eur. Phys. J. C **65**, 587-605 (2010) doi:10.1140/epjc/s10052-009-1218-5 [arXiv:0807.0894 [hep-th]].
 - [53] J. Bartels, L. N. Lipatov and A. Sabio Vera, "BFKL Pomeron, Reggeized gluons and Bern-Dixon-Smirnov amplitudes," Phys. Rev. D **80**, 045002 (2009) doi:10.1103/PhysRevD.80.045002 [arXiv:0802.2065 [hep-th]].
 - [54] L. N. Lipatov and A. Prygarin, "Mandelstam cuts and light-like Wilson loops in N=4 SUSY," Phys. Rev. D **83**, 045020 (2011) doi:10.1103/PhysRevD.83.045020 [arXiv:1008.1016 [hep-th]].
 - [55] L. N. Lipatov and A. Prygarin, "BFKL approach and six-particle MHV amplitude in N=4 super Yang-Mills," Phys. Rev. D **83**, 125001 (2011) doi:10.1103/PhysRevD.83.125001 [arXiv:1011.2673 [hep-th]].
 - [56] J. Bartels, L. N. Lipatov and A. Prygarin, "MHV amplitude for $3 \rightarrow 3$ gluon scattering in Regge limit," Phys. Lett. B **705**, 507-512 (2011) doi:10.1016/j.physletb.2011.09.061 [arXiv:1012.3178 [hep-th]].
 - [57] J. Bartels, A. Kormilitzin, L. N. Lipatov and A. Prygarin, "BFKL approach and $2 \rightarrow 5$ maximally helicity violating amplitude in $\mathcal{N} = 4$ super-Yang-Mills theory," Phys. Rev. D **86**, 065026 (2012) doi:10.1103/PhysRevD.86.065026 [arXiv:1112.6366 [hep-th]].